Int. J. Electrochem. Sci., 11 **(2016)** 6775 – 6790, doi: 10.20964/2016.08.33

International Journal of
ELECTROCHEMICAL
SCIENCE
www.electrochemsci.org

Electrochemical Analysis of 4-methyl-2-phenyl-imidazole Adsorbed on Cu

Matjaž Finšgar

University of Maribor, Faculty of Chemistry and Chemical Engineering, Smetanova ulica 17, 2000 Maribor, Slovenia
E-mail: matjaz.finsgar@um.si

Received: 27 February 2016 / *Accepted:* 18 March 2016 / *Published:* 7 July 2016

Herein, for the first time a detailed electrochemical analysis of Cu immersed in 3 wt.% NaCl containing 4-methyl-2-phenyl-imidazole (MePhI) as a corrosion inhibitor was performed. This analysis was carried out by means of cyclic voltammetry, chronopotentiometry, and electrochemical impedance spectroscopy (EIS). There was a special focus on EIS measurements. It was shown that MePhI significantly inhibits copper oxidation to Cu(I) and Cu(II). The system becomes more noble when Cu is immersed in MePhI-containing solution compared to non-inhibited solution. EIS measurements revealed that Cu in inhibited solution undergoes mixed kinetic-controlled and diffusion-controlled processes. A high corrosion inhibition effect was also proven after 180 days of immersion. Moreover, contact angle analysis showed that MePhI increases the hydrophobic character of the Cu surface.

Keywords: Copper, Corrosion Inhibitor, 4-methyl-2-phenyl-imidazole, Cyclic Voltammetry, Electrochemical Impedance Spectroscopy

1. INTRODUCTION

Electrochemistry can provide crucial information about the properties of electroactive species in solution or solid materials, for example the thermodynamics of redox processes, the kinetics of electron transfer, a representation of the properties of the surface structure and its phenomena by equivalent electrical circuits, and the passivation property of the material. This is especially useful in corrosion studies of metals in inhibited and non-inhibited solutions. Herein, the term inhibited solution means that the solution contains a very small amount (in mM) of dissolved organic compounds that adsorb on the surface and form in a certain manner a corrosion protective layer. The mechanism of the corrosion inhibitor action is in most cases not known as usually only empirical trial and error

experiments are performed. Electrochemical analysis in combination with a surface analysis of metals with adsorbed corrosion inhibitors (e.g. by employing the XPS, SIMS, AFM, and STM techniques), frequently provide vital information about the corrosion inhibitor mechanism. Using this fundamental knowledge, new corrosion inhibitor compounds can be developed, either by selecting from the known organic compounds which are not known to act as corrosion inhibitors or by the synthesis of completely new compounds based on knowledge about their structure/performance characteristics (e.g. if certain functional group act so as to improve performance) [1-9].

Herein, 4-methyl-2-phenyl-imidazole (MePhI) as a Cu corrosion inhibitor in 3 wt.% NaCl was investigated. In general, it is known that imidazoles are potential Cu corrosion inhibitors [10-17], however MePhI has not hitherto been investigated for any metallic material, except that detailed XPS analysis, 3D-profilometry, and standard electrochemical tests were previously [18]. It was shown that MePhI is an effective corrosion inhibitor for Cu in 3 wt.% NaCl solution and that it acts as an anodic type inhibitor. XPS measurements showed that the thickness of the MePhI surface layer formed after 1h of immersion is 0.3–0.5 nm (using the Tougaard thickness analysis method). Angle-resolved XPS measurements suggested that both the C and N atoms of the MePhI molecule are involved in the inhibitor surface bonding and it was suggested that MePhI molecules lie flat on the surface [18].

Recently, electrochemical analysis under similar experimental conditions was performed for 2-mercaptobenzoxazole (MBOH) [19], 2-mercaptobenzimidzole (MBIH) [14], 2-mercaptobenzothiazole (MBTH) [20], 3-amino-1,2,4-triazole (3-AT), and 1,2,4-triazole (TRI) [21] as Cu corrosion inhibitors in 3 wt.% NaCl. It was shown that Cu corrosion in MBOH- or MBIH- or MBTH-containing solutions followed mixed kinetic-controlled and diffusion-controlled processes [14, 19, 20]. For 3-AT and TRZ it was shown that differences in the growth kinetics in the initial stage of adsorption exist. TRZ growth was faster and linear, whereas for 3-AT it was slower and logarithmic, indicating that the 3-AT surface layer is denser, more compact, and more protective, and consequently more effective [21].

In this work, 3 wt.% NaCl was used as a medium wherein the properties of Cu were investigated as it was shown before that this medium induces highly corrosive conditions for Cu and therefore it is an attractive medium for such research [14, 19-21]. First, cyclic voltammetry experiments were performed to collect information about the oxidation and reduction properties of Cu in 3 wt.% NaCl solution with or without MePhI. This experiment was carried out immediately after the immersion of Cu in solution and therefore it provides information after short-term immersion periods. Moreover, by detailed analysis employing electrochemical impedance spectroscopy (EIS) measurements at different immersion periods, the mechanism of Cu corrosion was investigated. It revealed the surface phenomena of Cu corrosion in solution containing MePhI, in order to observe film formation on the Cu surface vs. time, and to measure the double layer, oxide and coating (adsorbed inhibitor) capacitance, and charge transfer resistance. Moreover, the thickness of the oxide layer and the diffusion process of the Cu species traveling through the surface layers were investigated. During the EIS measurements chronopotentiometric measurements were carried out to follow the change of E vs. t. Moreover, the corrosion inhibition effect of MePhI was also proven after 180 days of immersion. Finally, the hydrophobic character of the Cu surface was analysed after MePhI adsorption by contact angle analysis.

Hitherto, to the best of the author's knowledge, no such electrochemical, long-term mass loss and contact angle analysis of Cu in solution containing MePhI exists in the literature. In fact, the author was the first ever to mention the potential use of this compound as a corrosion inhibitor in a previous surface analytical study [18].

2. MATERIALS AND METHODS

2.1. Sample and solution preparations

Solution with 3 wt.% NaCl containing 1 mM MePhI was prepared with Milli-Q water with a resistivity of 18.2 MΩ cm. The use of 1 mM concentration is common in corrosion inhibitor studies at room temperature [14, 15, 18-20, 22]. NaCl (pro analysis) was purchased from Carlo Erba, Italy and MePhI (with a purity of 95.0 wt.% as specified by the supplier) from Sigma Aldrich, USA. Temper Half Hard 2-mm thick copper plate (with 99.999 wt.% Cu as specified by the supplier) was purchased from Goodfellow (Cambridge, UK), from which Cu samples were cut out in the shape of discs 15 mm in diameter and used for the electrochemical measurements, immersion tests, and for the determination of the contact angle. The Cu samples were first ground using a rotating device under a stream of water. First 1000-grit SiC paper was used and then 2400- and 4000-grit papers (provided by Struers, Ballerup, Denmark). To remove the particles resulting from grinding, the sample was rinsed with Milli-Q water between each paper change. Samples were ground in one direction until all imperfections were removed and the surface was covered with a uniform pattern of scratches. The grinding direction was changed four times by turning the sample 90° four times to minimize abrasion. Before each analysis, surfaces were checked under a microscope and if any scratches were still present, the preparation procedure was repeated. Finally, the samples were cleaned ultrasonically in a bath of 50% ethanol/50% Milli-Q water (by volume) and afterwards thoroughly rinsed with Milli-Q water and dried under a stream of air. The same preparation procedure has been used previously [14, 15, 19-21, 23-34].

2.2. Electrochemistry

A Gamry 600^{TM} potentiostat/galvanostat model was used for the electrochemical measurements. The instrument was controlled by the Gamry Framework program. As a working electrode, Cu discs (prepared as described above) were employed. They were embedded in a Teflon holder using a Teflon o-ring that exposed 1 cm^2 of the electrode to the solution. The holder was purchased from Princeton Applied Research (PAR). A three-electrode glass cell (PAR) was filled with 1 L solution. This cell was closed to air and under stagnant conditions at 25 °C during the electrochemical experiment, which was controlled by a thermostat. As reference and counter electrodes, a saturated calomel electrode (i.e. SCE, 0.2444 V vs. standard hydrogen electrode, SHE) and a platinum mesh were employed, respectively. The reference electrode was inserted in the Luggin capillary. For both the reference electrode and Luggin capillary, a porous glass frit (PAR G0300) was used [14, 19, 20].

Three different electrochemical experiments were carried out: cyclic voltammetry, chronopotentiometry, and EIS. For the cyclic voltammetry, the initial and final potentials were -0.8 V vs. SCE, and the switching potential was set at 1.0 V vs. SCE. This experiment was performed at a potential scan rate (v) of 10 mV/s [25]. Chronopotentiometry and EIS measurements were performed simultaneously. Chronopotentiometry measurements were carried out from the initial Cu immersion in the solution up to 100h of immersion. In between, EIS experiments were performed after 1, 3, 5, 10, 30, 50, and 100h of immersion. Every EIS experiment lasted approximately 30 minutes and was performed in a frequency range from 1 MHz to 5 mHz with 10 points per decade and a 10 mV (peak to peak) amplitude of the excitation signal at the open circuit potential, E_{oc}. The EIS data were interpreted on the basis of equivalent electrical circuits by modelling the measured response with electrical circuit elements, such as resistors, capacitors, and Warburg elements [14, 19, 20]. The fitting procedure of the EIS data was performed with Gamry's EChem Analyst software.

Three replicate measurements for every electrochemical experiment were performed. The possible presence of outliers in the EIS fitting procedure was checked with Grubbs' statistical test [35], but no outliers were detected. Moreover, no significant differences were observed with regard to the cyclic voltammetry and chronopotentiometic measurements. As a result, one of the three measurements is presented in the figures below [14, 19, 20, 24].

2.3. Immersion tests

Mass loss measurements were carried out in solutions with or without a 1 mM concentration of MePhI by weighing the mass of the samples before and after the exposure to the test solution. Immersion tests were performed in glass beakers containing 1 L of solution that were closed to the surrounding air. Samples were prepared according to the above-described procedure and subsequently immersed in the test solution. After 180 days of immersion, the specimens were taken from the solutions and cleaned by rinsing with Milli-Q water, brushing with a fibre-bristle brush, and immersion in an ultrasound bath [31]. Finally, the samples were rinsed again with Milli-Q water, dried under a stream of air and weighed. The same as for the electrochemical measurements described above, three such experiments were performed and the possible presence of outliers was checked with Grubbs' statistical test [35], but no outliers were detected.

2.4. Contact angle measurements

A OCA 35 Dataphysic (Filderstadt, Germany) instrument was employed for the contact angle (Θ) analysis. A Θ determination was made by analysing the image of the deionized water drop on the sample surface, where the Θ is determined as the angle between the surface plane and the droplet edge. The higher the Θ, the more the hydrophobic behaviour of the surface. Cu samples were immersed in non-inhibited solution and MePhI-inhibited solution for 1h, rinsed with Milli-Q water and dried under a stream of air. Three replicate measurements were performed in three different places of the Cu surface for each sample and three replicate sample preparations were performed for non-inhibited

solution and MePhI-inhibited solution. Therefore, 9 measurements were performed for Θ analysis in both cases.

3. RESULTS AND DISCUSSION

3.1. Cyclic voltammetry

Figure 1 shows cyclic voltammograms for Cu immersed in 3 wt.% NaCl solution with or without 1 mM MePhI. Voltammograms were measured immediately after Cu immersion in the solution, without any preconditioning (this type of analysis was performed by EIS as explained below). Therefore, the corrosion inhibition effectiveness of MePhI was checked in the first stage of this investigation for short-term immersion periods.

The measurement started at -0.8 V vs. SCE and progressed in the anodic direction. Copper in chloride medium oxidizes to Cu(I) forming CuCl (adsorbed on the Cu substrate) according to the first electrochemical reaction in Eq. 1. This process is indicated by the development of the A_1 current peak at 0.01 V vs. SCE in Fig. 1 for the Cu voltammogram measured in solution without MePhI (non-inhibited solution).

$$\mathrm{Cu} + \mathrm{Cl}^- \leftrightarrows \mathrm{CuCl}_{ads} + e^- \quad \textbf{(1)}$$

Next, the adsorbed CuCl chemically reacts with Cl^- to form a $CuCl_2^-$ complex (Eq. 2).

$$\mathrm{CuCl}_{ads} + \mathrm{Cl}^- \leftrightarrows \mathrm{CuCl}_2^- \quad \textbf{(2)}$$

This complex is soluble in aqueous media and can diffuse into the bulk solution or oxidize further by sweeping the applied potential to more positive potentials. The second electrochemical reaction is then:

$$\mathrm{CuCl}_2^- \leftrightarrows \mathrm{Cu}^{2+} + 2\mathrm{Cl}^- + e^- \quad \textbf{(3)}$$

The A_2 current peak represents this second electrochemical reaction in Fig. 1 at 0.14 V vs. SCE. Therefore, the mechanism of copper oxidation in chloride media can be described as ECE (electrochemical-chemical-electrochemical as the chemical and electrochemical reactions are commonly designated with letters C and E, respectively). However, the direct oxidation of $CuCl_{ads}$ to Cu^{2+} was also proposed (Eq. 4). This proposed mechanism would then be an EE mechanism.

$$\mathrm{CuCl}_{ads} \leftrightarrows \mathrm{Cu}^{2+} + \mathrm{Cl}^- + e^- \quad \textbf{(4)}$$

The relatively intense current plateau at potentials more positive than that for the A_2 current peak corresponds to the equilibrium between the formation of a poorly protective CuCl surface layer

and the dissolution of $CuCl_2^-$ complex [25]. In the cathodic direction, after the switching potential (at 1 V vs. SCE), only one cathodic peak (K_1) is observed at -0.18 V vs. SCE, corresponding to CuCl reduction [33] (because Cu^{2+} species are soluble and diffuse into the solution, and thus do not remain on the surface) [36, 37].

When Cu is immersed in 3 wt.% NaCl containing 1 mM MePhI a significant reduction of the A_1 current peak (designated as A_1^*) is noticed in Fig. 1. Therefore, MePhI significantly inhibits Cu(I) formation. This peak is also transferred to more positive potentials compared with the measurements for the non-inhibited solution (A_1* vs. A_1). This can also be an indication that Cu(I)-MePhI complex is formed, which is responsible for the corrosion inhibition. The formation of Cu(I)-azole-type complexes are common when Cu is immersed in azole-containing solutions [16, 17, 38]. Moreover, a Cu(I)-MePhI connection was also predicted before using the XPS measurements [18]. By increasing the potential in the anodic direction, an A_2* current peak develops (inset in Fig. 1), which is significantly less intense that that for the non-inhibited solution and also transferred to more positive potentials (A_2* vs. A_2). This again proves the high corrosion inhibition effectiveness of the MePhI compound because significantly less Cu(II) was formed compared to the measurement for the non-inhibited solution. In the potential region more positive than the potential for the A_2* current peak, a significantly less intensely expressed current plateau is noticed compared to the measurement for the non-inhibited solution. This again signifies that a highly effective MePhI surface layer was formed, which inhibits Cu oxidation.

In the reverse direction in the case of solution containing MePhI, one cathodic peak is present (designated as K_1*). This peak is significantly less intense compared with the measurement for the non-inhibited solution (K_1* vs. K_1) as less Cu(I) was formed in the anodic cycle when MePhI was present. Moreover, this peak is located at more negative potentials compared with that for the non-inhibited solution. The higher potential difference between the anodic and cathodic peaks than the potential difference for the measurement in the non-inhibited solution indicates an irreversible reaction in the former case. This is connected with the MePhI/Cu system being highly resistive to transferring the electron to the electroactive species in solution.

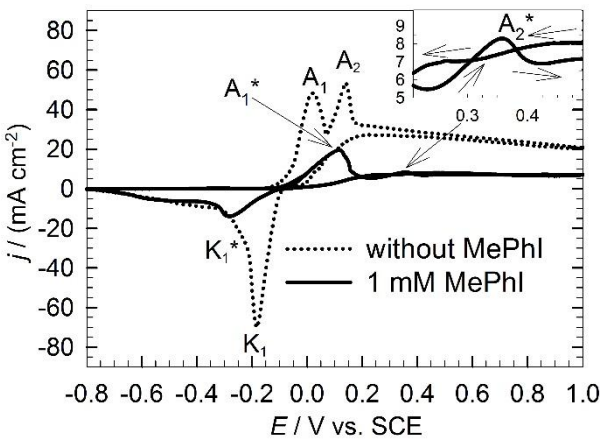

Figure 1. Cyclic voltammograms for Cu in 3 wt.% NaCl with or without 1 mM MePhI.

3.2. Chronopotentiometric measurements

Figure 2 shows the *E* vs. *t* measurements for Cu immersed in 3 wt.% NaCl solution that contained 1 mM MePhI. The measurements were carried out over 100h of immersion, starting immediately after the Cu electrode was immersed in the solution. During the Cu immersion after 1, 3, 5, 10, 30, and 50h, EIS measurements were performed (also after 100h of immersion, see below). That is why the chronopotentiometric curve is discontinuous in Fig. 2 (the arrows represent these immersion times). A clear indication that EIS is a non-destructive method is the fact that after EIS measurements the Cu material was not significantly changed compared to the condition of the Cu material before the EIS measurement, because the potential before and after the EIS measurement remained virtually the same (a change of only a few mV can be observed). If the sinusoidal EIS polarization had a significant impact on the material, the surface conditions would change and consequently the corrosion potential developed on the surface would change.

Figure 2 shows that the potential significantly increases immediately after the immersion of the Cu electrode in the solution (this was the case for all 3 measurements, only 1 is shown herein). Subsequently, it drops a bit and in the period between 1–10h of immersion it becomes relatively constant. After 10h of immersion it starts to increase and continues up to 100h of immersion, reaching a value of -0.1689 V (Fig. 2). For comparison, the corrosion potential of Cu after 100h of immersion in pure (without any inhibitor) 3 wt.% NaCl solution is -0.2628 V. Therefore, the presence of MePhI in the solution makes the system more noble compared with the system that did not contain MePhI (the corrosion potential shifted to more positive potentials).

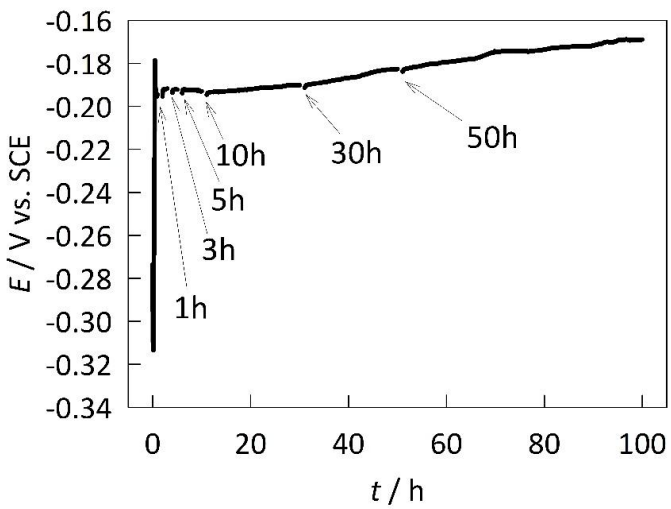

Figure 2. Chronopotentiometric measurements of Cu in 3 wt.% NaCl containing 1 mM MePhI.

3.3. Electrochemical impedance spectroscopy measurements

Figure 3 shows EIS measurements at different immersion periods over 100h of immersion for Cu in 3 wt.% NaCl containing 1 mM MePhI. The EIS spectra after relatively long immersion periods

reveal if significant rearrangements of the surface layers occur at different immersion periods (molecule desorption/adsorption, a change in molecule orientation, a change in the MePhI surface layer and oxide layer thickness).

In the $|Z|$ *vs.* f spectra (Figs. 3b), the horizontal amplitude is developed in the highest frequency region (Z and f stand for impedance and frequency, respectively). Simultaneously, the phase angle tends towards 0° with increasing f (Figs. 3c). This behaviour describes an uncompensated resistance R_Ω. In the high frequency region (between 10–100 kHz, which is at lower frequencies than that representative for R_Ω), a peak can be noticed in the phase angle Bode plot (Fig. 3c), indicating the capacitive behaviour of a certain relaxation process. In the middle frequency region, the slope of the curve in Fig. 3b is different than that for the high frequency region for all measurements (the most significant difference between the EIS spectra occurs in the case of the measurement after 100h of immersion compared with the measurements taken after shorter immersion periods). This may represent the presence of another relaxation process. In the low frequency region at about 0.1 Hz, another expressed peak can be noticed in the phase angle Bode plot (Fig. 3c), indicating another relaxation process. Therefore, at least three relaxation processes can be taken into account for the detailed analysis of the EIS spectra (which is performed below).

In the low f region of the EIS spectra, Z is usually independent of f in the $|Z|$ *vs.* f spectrum, reaching the so-called dc limit when $|Z| \approx R_p$ – polarisation resistance, because $|Z|=\sqrt{Z_{real}^2 + Z_{img}^2}$ and $\lim_{f\to 0}(Z_{real})_{E=E_{oc}} = R_p + R_\Omega$ and $\lim_{f\to 0}(Z_{img})=0$. Z_{real} and Z_{img} are the real and imaginary components of the impedance [14]. Polarization resistance is a measure of how the metal resists transferring electrons to the electroactive species in solution. The higher it is, the more resistant the system is to general corrosion. However, in Fig. 3b the horizontal amplitude at low f was not developed for all measurements, most likely due to the diffusion process and another process describing the adsorption/desorption process of MePhI on the Cu surface (Fig. 3b). Therefore, four relaxation processes will be taken into account in the EIS fitting procedure, which is given below.

By comparing the Cu spectra of the non-inhibited 3 wt.% NaCl presented previously [14] with the MePhI-treated Cu, the low f resistive region is transferred by approximately 2 orders of magnitude to the higher $|Z|$ in the $|Z|$ *vs.* f spectrum (Fig. 3b). This clearly indicates the corrosion inhibition effectiveness of MePhI compound. Moreover, by comparing the above-presented EIS spectra of MBOH- and MBTH-treated Cu in the same system as herein, the low f resistive region is at similar $|Z|$ in the $|Z|$ vs. f spectrum for measurements up to 50h of immersion, indicating the similar corrosion inhibition effect of these molecules. However, after 100h of immersion MBOH and MBTH induce a more resistive system than MePhI, as indicated by the higher $|Z|$ [19, 20]. An even more resistive system compared with the system containing these three molecules was found before for MBIH after from 1h up to 100h of Cu immersion [14].

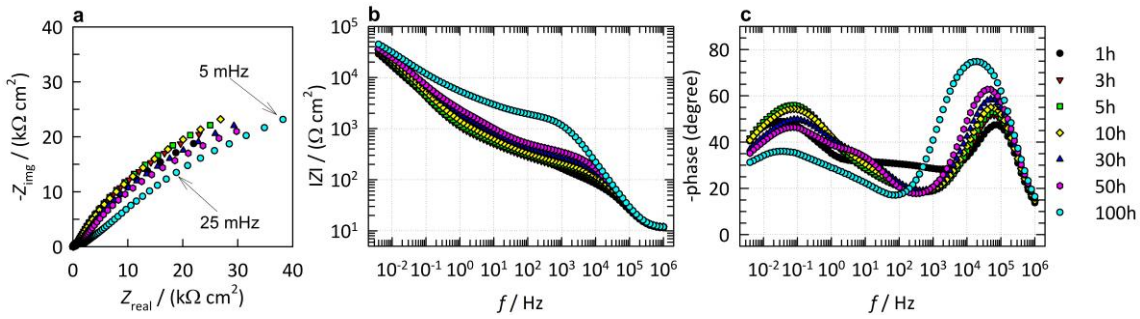

Figure 3. EIS measurements for Cu in 3 wt.% NaCl containing 1 mM MePhI measured after 1, 3, 5, 10, 30, 50, and 100h of immersion: a) Nyquist and b, c) Bode plots.

As mentioned above, in the EIS fitting procedure four relaxation processes were taken into account by employing the EEC (equivalent electrical circuit) model in Fig. 4 using a combination of resistance (R) and capacitance elements (Q, Eq. 5) in series with R_Ω. R_Ω is constant during the measurement (it should not change significantly during 100h of immersion if corrosion is not significant – if it were significant it would increase ion content in the solution) and represent ohmic resistance between the electrode surface and the reference electrode (the largest part of R_Ω originates from the solution resistance). The R_Ω values reported herein in Table 1 are 2–3 Ω higher than reported before [14, 19, 20]. This is connected with the use of ceramic frits in the present case, which seem to be more resistive (previously a Vycor frit was employed). It was found that by using a ceramic frit instead of a Vycor frit, lower phase angle values (very close to 0°) at high frequencies were recorded, whereas a Vycor frit induced phase angles of about 5–20°.

A non-ideal capacitance C is represented by the symbol Q (CPE, constant phase element) with varying n. The impedance of the CPE is given by [39]:

$$Z(\mathrm{CPE}) = (Q(j\omega)^n)^{-1} \quad \textbf{(5)}$$

When $n = 1$, the CPE describes an ideal capacitor. For $0.5 < n < 1$, the CPE describes the distribution of the dielectric relaxation times in the frequency space. A Warburg impedance is characteristic when $n = 0.5$ [19, 39].

For demonstration, the frequencies representing the four relaxation processes are designated as black rectangles in Fig. 5a for the measurement after 1h of immersion (calculated as f=1/(2πRC)). This is just one of the possible EEC models that can be used for the present system. However, other EEC models were also employed, but the fitting procedure resulted in a higher χ^2 (as defined in Eq. 6), which is a measure of the fitting goodness, which is defined as:

$$\boldsymbol{\chi^2} = \sum_{i=1}^{N} \frac{[(a_i - Z_i')^2 + (b_i - Z_i'')^2]}{\sigma_i^2} \quad \textbf{(6)}$$

$$\sigma_i = r\sqrt{a_i^2 - b_i^2}$$

The experimental data point is [ω_i, a_i, b_i], the calculated data point is [ω_i, Z_i', Z_i"], r is a fraction of the modulus and determined as $\chi^2_{\min} \approx r^2$, and N is the number of data points. A higher χ^2 value represents the worst fit [14, 19, 20]. The χ^2 values in the fitting procedure were between $3.8\cdot10^{-4}$ and $5.0\cdot10^{-4}$, indicating the appropriateness of the ECC used. The χ^2 values and fitted data are given in Table 1.

For comparison, it was previously demonstrated conclusively that Cu in pure chloride aqueous media without any corrosion inhibitor exhibits three relaxation processes and which were represented by $R_\Omega(Q_1(R_1(Q_2(R_2(Q_3R_3))))$ or $R_\Omega(Q_1(R_1(Q_{dl}(R_{ct}W)))$ nested EECs [40]. Herein, another relaxation process is included in the EIS analysis, representing the properties related to the inhibitor surface layer on the Cu. This kind of nested relaxation processes in the EEC models are commonly employed in the EIS fitting procedure for passive and coated metals [39, 41-44].

The high-frequency relaxation process R_1Q_1 (the frequency for that process was calculated to be approximately 1–22.9 kHz for 1-100h of immersion, f=1/(2πRC)) is related to the properties of the passive layer on the surface. The passive layer is the Cu_2O oxide layer on the copper surface (most likely below the MePhI layer). The second relaxation process, R_2Q_2 (at approximately 0.08–1.63 kHz for 1–100h of immersion), is related to the properties of charge transfer resistance and double-layer capacitance, described with R_2 and Q_2 in Fig. 4 and Table 1, respectively. The n values for Q_1 and Q_2 are close to 1 (and higher than n_4), describing well the capacitive behaviours of the passive layer and the double-layer. The third process, R_3Q_3, at calculated f of between 0.14–6.14 Hz for 1-100h of immersion, is related to the diffusion of ionic species that travel from the substrate to the bulk solution. This assumption is based on ascertained n_3 values in Table 1, which are close to 0.5 (an n of 0.5 is representative for the diffusion process). The low f R_4Q_4 process is related to the adsorption/desorption (calculated f at approximately 1.9–11.6 mHz for 1–100h of immersion) of the MePhI on the Cu surface. The calculated C_4 from Q_4 is 100-1000 times higher than C_2, which describes double-layer capacitance (see Fig. 6), and corresponds to the adsorption capacitance [19, 20, 39]. R_1 and R_4 represent resistances at the substrate-electrolyte interface covered by the Cu_2O and MePhI, respectively. These surface layers comprise pockets filled with an electrolyte solution that are ion conducting paths, where the electrolyte solution is very different than the bulk solution outside of these surface layers. Consequently, these R values are significantly higher (surface layers also restrict ion movement, which significantly contribute to higher R).

Polarisation resistance (R_p) is commonly employed as a measure of how the metal resists against general corrosion. The higher this value is, the more resistant the system is. R_p is the sum of all resistances ascertained in the fitting procedure ($R_p = R_1 + R_2 + R_3 + R_4$). As seen in Table 1, the largest contribution to the R_p value comes from R_4. Therefore, the adsorption of the MePhI on the surface is crucial for the corrosion inhibition effect. This might seem straightforward at first sight, but a corrosion inhibitor can also act in a way so as to reinforce the oxide layer below the topmost inhibitor surface layer [45], which provides corrosion protection (such that not only the inhibitor surface layer is responsible for corrosion protection).

Fig. 6 shows calculated capacitance (C) values by employing the relation $C_x=(R_xQ_x)n_x/R_x$ and the fitted data given in Table 1 [19, 20, 39]. The C_1 values describing the capacitance of the passive layer (oxide) do not change significantly in the immersion period from 1h to 100h, indicating that the

oxide layer is stable – the thickness of that layer does not increase or decrease (as the thickness is inversely proportional to the capacitance, assuming a perfect parallel-plate condenser of a homogeneous oxide layer, because everything else in $d_{ox}=(\varepsilon_0\varepsilon A)/C_1$ is constant). The permittivity of the vacuum is ε_0 ($8.85\cdot10^{-14}$ F/cm), ε is the dielectric constant, A is the geometric area of the electrode (1 cm^2), and d_{ox} is the thickness of the oxide layer. The calculated C_1 value for 1h of immersion is 8.4×10^{-8} F cm^{-2}. Using this value and by taking into account two limiting ε as 10 and 40 (which is usual for metal oxides [19, 46]), the d_{ox} value is between 1.05 and 4.21 nm. The oxide layer is most likely below the MePhI surface layer. Using the Tougaard method, the thickness of the MePhI surface layer was determined previously to be 0.3–0.5 nm [18]. By taking these limiting values of both surface layers (oxide and inhibitor), the total thickness of the surface layers on the pure copper is estimated to be 1.35–4.71 nm.

The double-layer capacitance C_2 changes the most for the immersion period from 1h to 10h. The capacitance is connected with the active part of the surface area (the higher the area, the higher the capacitance) – and therefore not the parts covered by the surface layers [47]. As the C_2 decreases over the first 10h of immersion, this is most likely connected with an MePhI adsorption process covering the active surface. In the immersion period from 10 to 100h, it is constant as the MePhI adsorption process ceases. Q_3 represents diffusion (n_3 is close to 0.5, see above), therefore the capacitance calculation is not relevant. The values describing the capacitance of the inhibitor surface layer (C_4 for the R_4Q_4 relaxation) increase by increasing the immersion time up to 100h of immersion. This increment is the most pronounced within the first 5h of immersion. The increment might indicate that the thickness of the inhibitor surface layer decreases with increasing immersion time (the same C vs. layer thickness relationship applies as explained above for the passive layer – the first relaxation process), indicating desorption of the inhibitor.

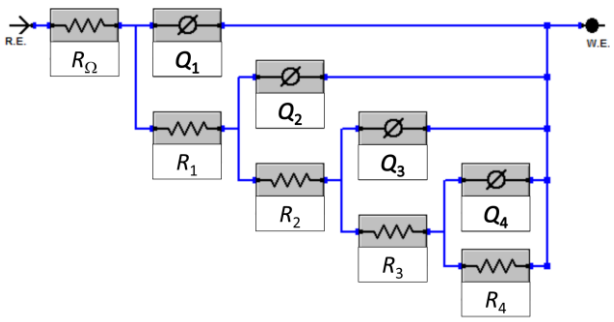

Figure 4. The $R_\Omega(Q_1(R_1(Q_2(R_2(Q_3(R_3(R_4Q_4)))))))$ model used to fit the experimental EIS spectra obtained after 1, 3, 5, 10, 30, 50, and 100h of immersion. This model induced the lowest χ^2. R.E. and W.E. represent the reference and working electrodes, respectively.

What is meant by desorption is that molecules that are adsorbed on the very first layer or from the following layers are desorbed and not those that were adsorbed directly on the Cu substrate (otherwise C_2 would change). The thickness of the surface layer is not connected with the surface coverage, as this is constant after 10h of immersion (predicated above by the interpretation of C_2 values).

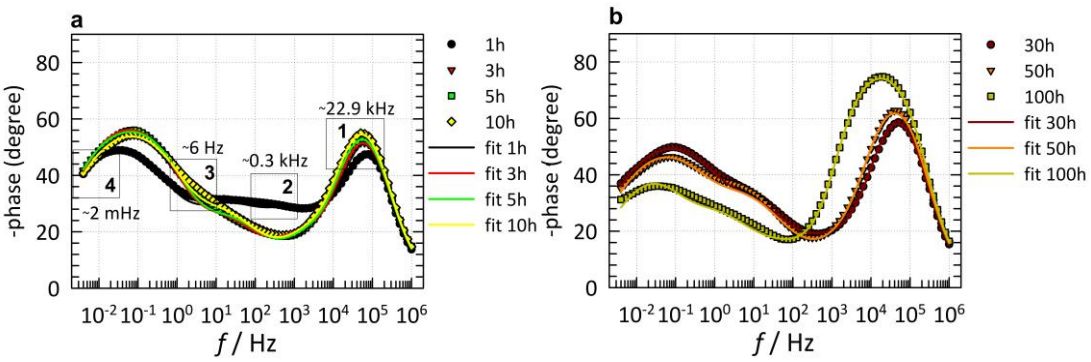

Figure 5. Measured (dotted) and fitted (solid lines) phase angle EIS spectra using the EEC model in Fig. 4 for the measurements after a) 1h, 3h, 5h, and 10h and b) 30h, 50h, and 100h of immersion.

Table 1. Fitted EIS parameters using the EEC model describing four relaxation processes in Fig. 4 for Cu in 3 wt.% NaCl containing 1 mM MePhI after 1h, 3h, 10h, 30h, 50h, and 100h of immersion. Units: χ^2 [$\times 10^{-3}$], R_Ω [Ω cm^2], R_1, R_2, R_3, and R_4 [kΩ cm^2], Q_1, Q_2, Q_3, and Q_4 [$\mu\Omega^{-1}$ cm^{-2} s^n], $R_p = R_1 + R_2 + R_3 + R_4$ [kΩ cm^2].

Immersion time [h]	χ^2	R_Ω	Q_1	n_1	R_1	Q_2	n_2	R_2	Q_3	n_3	R_3	Q_4	n_4	R_4	R_p
1	0.49	10.5	0.169	0.92	1.66	7.29	0.83	0.83	75.81	0.55	14.18	97.0	0.73	70.71	87.38
3	0.41	10.5	0.226	0.90	0.32	3.09	0.89	0.10	103.80	0.59	3.98	97.1	0.68	77.73	82.13
5	0.42	10.6	0.241	0.90	0.22	3.93	0.89	0.12	114.10	0.60	2.33	94.5	0.69	83.38	86.05
10	0.38	10.7	0.263	0.90	0.16	3.48	0.88	0.09	126.90	0.62	1.19	135.2	0.74	89.78	91.22
30	0.56	10.6	0.295	0.89	0.14	3.70	0.89	0.07	135.10	0.62	0.82	175.4	0.76	86.02	87.06
50	0.46	10.4	0.309	0.89	0.13	9.21	0.80	0.11	136.30	0.65	0.74	206.3	0.76	70.91	71.89
100	0.50	10.5	0.223	0.92	0.08	20.64	0.68	0.29	82.07	0.62	1.25	233.9	0.67	81.97	83.59

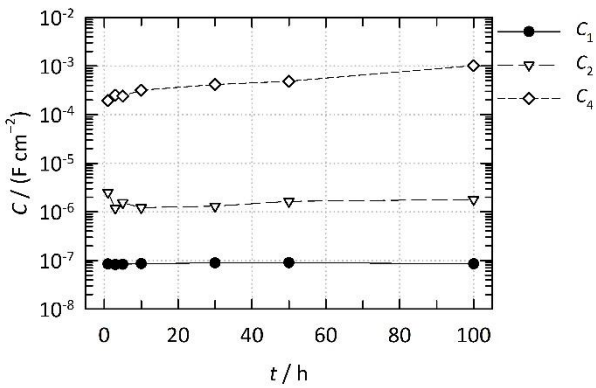

Figure 6. Calculated C values according to $C_x=(R_xQ_x)n_x/R_x$ using the ascertained Q, R, and n values in the fitting procedure in Table 1.

However, the change of C_4 vs. t is not as significant as found before for MBOH [19] and MBTH [20]. Therefore, in the present case the MePhI does not undergo a significant rearrangement during 100h of immersion, which also does not significantly change the corrosion inhibition effectiveness of the MePhI over 100h of immersion, as seen from the R_p values in Table 1.

3.4. Mass loss measurements

MePhI corrosion inhibition effectiveness was also tested after a relatively long-term immersion period, i.e. 6 months (180 days). The average mass loss (3 replicate measurements, outliers were checked with Grubbs' statistical test [35], but no outliers were detected) was calculated for the non-inhibited 3 wt.% NaCl solution (Δm_0) and 3 wt.% solution containing 1 mM MePhI (Δm_i). From the so obtained average mass losses, the inhibition effectiveness η was calculated to be 98.8% according to Eq. (7):

$$\eta = 100\frac{\Delta m_0 - \Delta m_\mathrm{i}}{\Delta m_0} \quad \textbf{(7)}$$

Such a high % value does not mean that Cu does not corrode in MePhI-containing 3 wt.% NaCl, but that the mass loss was significantly higher for the non-inhibited solution compared to the MePhI-inhibited solution. This again proves that MePhI is also a highly effective corrosion inhibitor after long-term immersion periods.

3.5. Contact angle analysis

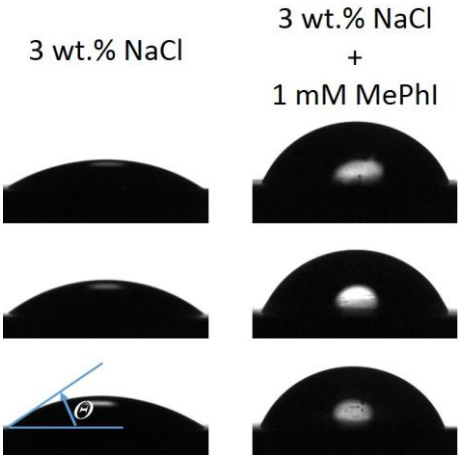

Figure 7. The shapes of the deionized water droplets (one out of three samples) for the contact angle (Θ) analysis on the Cu surfaces previously immersed for 1h in non-inhibited solution and MePhI-inhibited solution (three replicate measurements for both cases).

Figure 7 shows the shapes of deionized water droplets on the surfaces after preparing samples in non-inhibited solution and MePhI-inhibited solution. An immersion time of 1h was chosen to investigate the surface characteristics on the very first inhibitor layers as longer immersion periods would result in the formation of crystallites on the surface, which are not primarily responsible for the corrosion inhibition effect [18, 25]. The average Θ value (9 measurements) of the measurements for the 3 samples (3 different spots were analysed) immersed in non-inhibited 3 wt.% NaCl was 43.0°±4.4° (95% confidence interval, determined as $\pm ts/\sqrt{n}$, t – Student's t-distribution, s – standard

deviation, n – number of measurements [48]). The average Θ value for the same analysis of the Cu samples immersed in 3 wt.% NaCl containing 1 mM MePhI was 68.7°±2.9°. The Θ increase for the inhibited compared to the non-inhibited solution is also clearly seen in Fig. 7 (one example of how the Θ is determined is demonstrated for the non-inhibited solution). Therefore, after adsorption from 3 wt.% NaCl, MePhI increases the hydrophobic character of the Cu surface. This increment also explains the corrosion inhibition ability of that compound as the amount of electrolyte solution (water solution) in contact with the Cu surface is lower for the inhibited sample compared to the non-inhibited sample, which results in mitigating corrosion.

4. CONCLUSIONS

In this work an electrochemical study of Cu in 3 wt.% NaCl solution was performed using cyclic voltammetry, chronopotentiometry, electrochemical impedance spectroscopy. Moreover, a long-term immersion tests and contact angle analysis were performed. The main findings are the following:

- Short-term immersion tests performed by cyclic voltammetry measurements showed a significant reduction in both anodic and cathodic peaks for Cu when MePhI was present in solution compared to the non-inhibited solution. Moreover, the higher potential difference between the anodic and cathodic peaks for the inhibited compared to the non-inhibited system demonstrates irreversible reactions in the former case due to the resistive MePhI/Cu system.
- The system containing MePhI is more noble compared to the system without MePhI, as determined by chronopotentiometric measurements.
- Four relaxation processes were determined with detailed analysis of the EIS spectra characterizing the properties of the copper oxide layer, charge-transfer resistance and double-layer capacitance, the diffusion process, and a process describing the adsorption/desorption properties of MePhI. Therefore, the corrosion of Cu immersed in MePhI-inhibited solution follows mixed diffusion-controlled and kinetic-controlled processes.
- Using the EIS fitting procedure, the thickness of the copper oxide layer formed after 1h of immersion was estimated to be between 1.05 and 4.21 nm.
- MePhI is an effective corrosion inhibitor after a long-term immersion period, i.e. 180 days.
- MePhI increases the hydrophobic character of the surface, as determined by contact angle measurements.

ACKNOWLEDGMENTS
This work was supported by the Slovene Research Agency (Grant No. Z1-6737)

References

1. K. Krishnaveni, J. Ravichandran, *J. Electroanal. Chem.*, 735 (2014) 24.

2. F. Caprioli, A. Martinelli, V. Di Castro, F. Decker, *J. Electroanal. Chem.*, 693 (2013) 86.
3. B.M. Mistry, S.K. Sahoo, S. Jauhari, *J. Electroanal. Chem.*, 704 (2013) 118-129.
4. S. Neodo, D. Carugo, J.A. Wharton, K.R. Stokes, *J. Electroanal. Chem.*, 695 (2013) 38.
5. A. Romeiro, C. Gouveia-Caridade, C.M.A. Brett, *J. Electroanal. Chem.*, 688 (2013) 282.
6. R. Fuchs-Godec, G. Žerjav, *Corros. Sci.*, 97 (2015) 7.
7. G. Žerjav, I. Milošev, *Corros. Sci.*, 98 (2015) 180.
8. R. Fuchs-Godec, G. Žerjav, *Acta Chim. Slov.*, 56 (2009) 78.
9. R.F.V. Villamil, P. Corio, S.M.L. Agostinho, J.C. Rubim, *J. Electroanal. Chem.*, 472 (1999) 112.
10. Y. I. Kuznetsov, L. P. Kazansky, I. A. Seljaninov, D. Starosvetsky, Y. Ein-Eli, *Electrochem. Solid St.*, 12 (2009) C21.
11. B. Assouli, Z.A. Ait Chikh, H. Idrissi, A. Srhiri, *Polymer*, 42 (2001) 2449.
12. K.T. Carron, M.L. Lewis, J. Dong, J. Ding, G. Xue, Y. Chen, *J. Mater. Sci.*, 28 (1993) 4099.
13. D. Chadwick, T. Hashemi, *Surf. Sci.*, 89 (1979) 649.
14. M. Finšgar, *Corros. Sci.*, 72 (2013) 82.
15. M. Finšgar, *Corros. Sci.*, 72 (2013) 90.
16. M.M. Antonijević, M.B. Petrović, *Int. J. Electrochem. Sci.*, 3 (2008) 1.
17. M.M. Antonijević, S.M. Milić, M.B. Petrović, *Corros. Sci.*, 51 (2009) 1228.
18. M. Finsgar, *Anal. Methods*, 7 (2015) 6496.
19. M. Finšgar, D. Kek Merl, *Corros. Sci.*, 80 (2014) 82.
20. M. Finšgar, D. Kek Merl, *Corros. Sci.*, 83 (2014) 164.
21. M. Finšgar, *Corros. Sci.*, 77 (2013) 350.
22. M. Finšgar, J. Jackson, *Corros. Sci.*, 86 (2014) 17.
23. M. Finšgar, J. Kovač, I. Milošev, *J. Electrochem. Soc.*, 157 (2010) C52.
24. M. Finšgar, I. Milošev, *Corros. Sci.*, 52 (2010) 2430.
25. M. Finšgar, I. Milošev, *Mater. Corros.*, 62 (2011) 956.
26. A. Kokalj, S. Peljhan, M. Finšgar, I. Milošev, *J. Am. Chem. Soc.*, 132 (2010) 16657.
27. M. Finšgar, *Corros. Sci.*, 68 (2013) 51.
28. M. Finšgar, S. Fassbender, S. Hirth, I. Milošev, *Mater. Chem. Phys.*, 116 (2009) 198.
29. M. Finšgar, S. Fassbender, F. Nicolini, I. Milošev, *Corros. Sci.*, 51 (2009) 525.
30. M. Finšgar, S. Peljhan, A. Kokalj, J. Kovač, I. Milošev, *J. Electrochem. Soc.*, 157 (2010) C295.
31. M. Finšgar, J. Jackson, *Mater. Corros.*, 66 (2015) 1299.
32. M. Finšgar, A. Lesar, A. Kokalj, I. Milošev, *Electrochim. Acta*, 53 (2008) 8287.
33. M. Finšgar, I. Milošev, B. Pihlar, *Acta Chim. Slov.*, 54 (2007) 591.
34. A. Kokalj, N. Kovačević, S. Peljhan, M. Finšgar, A. Lesar, I. Milošev, *ChemPhysChem*, 12 (2011) 3547.
35. D.L. Massart, B.G.M. Vandeginste, L.M.C. Buydens, S.D. Jong, P.J. Lewi, J. Smeyers-Verbeke, Handbook of Chemometrics and Qualimetrics: Part A, Elsevir, Amsterdam, 1997.
36. H.P. Lee, K. Nobe, *J. Electrochem. Soc.*, 133 (1986) 2035.
37. H. Otmacic, J. Telegdi, K. Papp, E. Stupnisek-Lisac, *J. Appl. Electrochem.*, 34 (2004) 545-550.
38. S.M. Milić, M.M. Antonijević, *Corros. Sci.*, 51 (2009) 28.
39. I.D. Raistrick, D.R. Franceschetti, J.R. Macdonald, Impedance Spectroscopy Theory, Experiment, and Application, 2nd Edition, John Wiley&Sons, Inc., Hoboken, New Jersey, 2005.
40. Y. Van Ingelgem, E. Tourwé, J. Vereecken, A. Hubin, *Electrochim. Acta*, 53 (2008) 7523.
41. A. Kocijan, D.K. Merl, M. Jenko, *Corros. Sci.*, 53 (2011) 776.
42. J.M. Atebamba, J. Moskon, S. Pejovnik, M. Gaberscek, *J. Electrochem. Soc.*, 157 (2010) A1218.
43. B. Guitian, X.R. Novoa, B. Puga, *Electrochim. Acta*, 56 (2011) 7772.
44. D.K. Merl, P. Panjan, M. Cekada, M. Macek, *Electrochim. Acta*, 49 (2004) 1527.
45. M. Finšgar, I. Milošev, *Corros. Sci.*, 52 (2010) 2737.
46. E.M. Orazem, B. Tribollet, Electrochemical Impedance Spectroscopy, John Wiley & Sons, Inc., Hoboken, New Jersey, 2008.

47. D. Kek Merl, P. Panjan, J. Kovač, *Corros. Sci.*, 69 (2013) 359.
48. D.L. Massart, B.G.M. Vandeginste, L.M.C. Buydens, S.D. Jong, P.J. Lewi, J. Smeyers-Verbeke, Handbook of Chemometrics and Qualimetrics: Part A, Elsevir, Amsterdam, 1997.

© 2016 The Authors. Published by ESG (www.electrochemsci.org). This article is an open access article distributed under the terms and conditions of the Creative Commons Attribution license (http://creativecommons.org/licenses/by/4.0/).